Kinematics of large scale asymmetric folds and associated smaller scale brittle–ductile structures in the Proterozoic Somnur Formation, Pranhita–Godavari valley, south India

Gautam Ghosh[1*] and Dilip Saha[2]

[1] *Department of Geology, Presidency College, Kolkata 700 073, India.*
[2] *Geological Studies Unit, Indian Statistical Institute, Kolkata 700 035, India.*
[*] *e-mail: gautam_0262@rediffmail.com*

The development of structural elements and finite strain data are analysed to constrain kinematics of folds and faults at various scales within a Proterozoic fold-and-thrust belt in Pranhita–Godavari basin, south India. The first order structures in this belt are interpreted as large scale buckle folds above a subsurface decollement emphasizing the importance of detachment folding in thin skinned deformation of a sedimentary prism lying above a gneissic basement. That the folds have developed through fixed-hinge buckling is constrained by the nature of variation of mesoscopic fabric over large folds and finite strain data. Relatively low, irrotational flattening strain (X:Z – 3.1–4.8, $k < 1$) are associated with zones of near upright early mesoscopic folds and cleavage, whereas large flattening strain (X:Z – 3.9–7.3, $k < 1$) involving noncoaxiality are linked to domains of asymmetric, later inclined folds, faults and intense cleavage on the hanging wall of thrusts on the flanks of large folds. In the latter case, the bulk strain can be factorized to components of pure shear and simple shear with a maximum shearing strain of 3. The present work reiterates the importance of analysis of minor structures in conjunction with strain data to unravel the kinematic history of fold-and-thrust belts developed at shallow crustal level.

1. Introduction

Large scale asymmetric folds associated with contractional faults at various scales are often found to be an integral part of fold-and-thrust belts. Various kinematic models have been proposed to explain these linked fold-and-thrust structures *viz.*, fault-bend folds, fault-propagation folds, detachment folds, displacement-gradient folds and break thrust folds (Willis 1893; Suppe 1983; Jamison 1987; Suppe and Medwedeff 1990; Fischer *et al* 1992; Homza and Wallace 1995; Thorbjornsen and Dunne 1997). Most of these models, barring detachment and break thrust folds, assume that the fold structures evolve as migrating hinge kink folds deformed by slip on bedding planes between kink band boundaries. The inherent weakness in these models is the assumption that the folds are passive folds, their geometry being entirely controlled by movements on associated faults. The applicability of these models is thus limited in the case of fixed hinged buckle folds where layering plays an important role in controlling ultimate fold geometry and development of associated minor structures.

Two end-member folding mechanisms namely fixed-hinge folding (involving limb rotation about fixed axial surfaces, e.g., De Sitter 1956) and active-hinge folding (involving lateral migration of active axial surfaces, e.g., Suppe 1983) are invoked to explain finite fold development. Any inference about fold kinematics is based on the analysis of distributions of diagnostic deformation features (Stewart and Alvarez 1991; Fischer *et al*

Keywords. Kinematic history; asymmetric buckle folds; thrust related folding; Proterozoic Somnur Formation.

J. Earth Syst. Sci. **114**, No. 2, April 2005, pp. 125–142

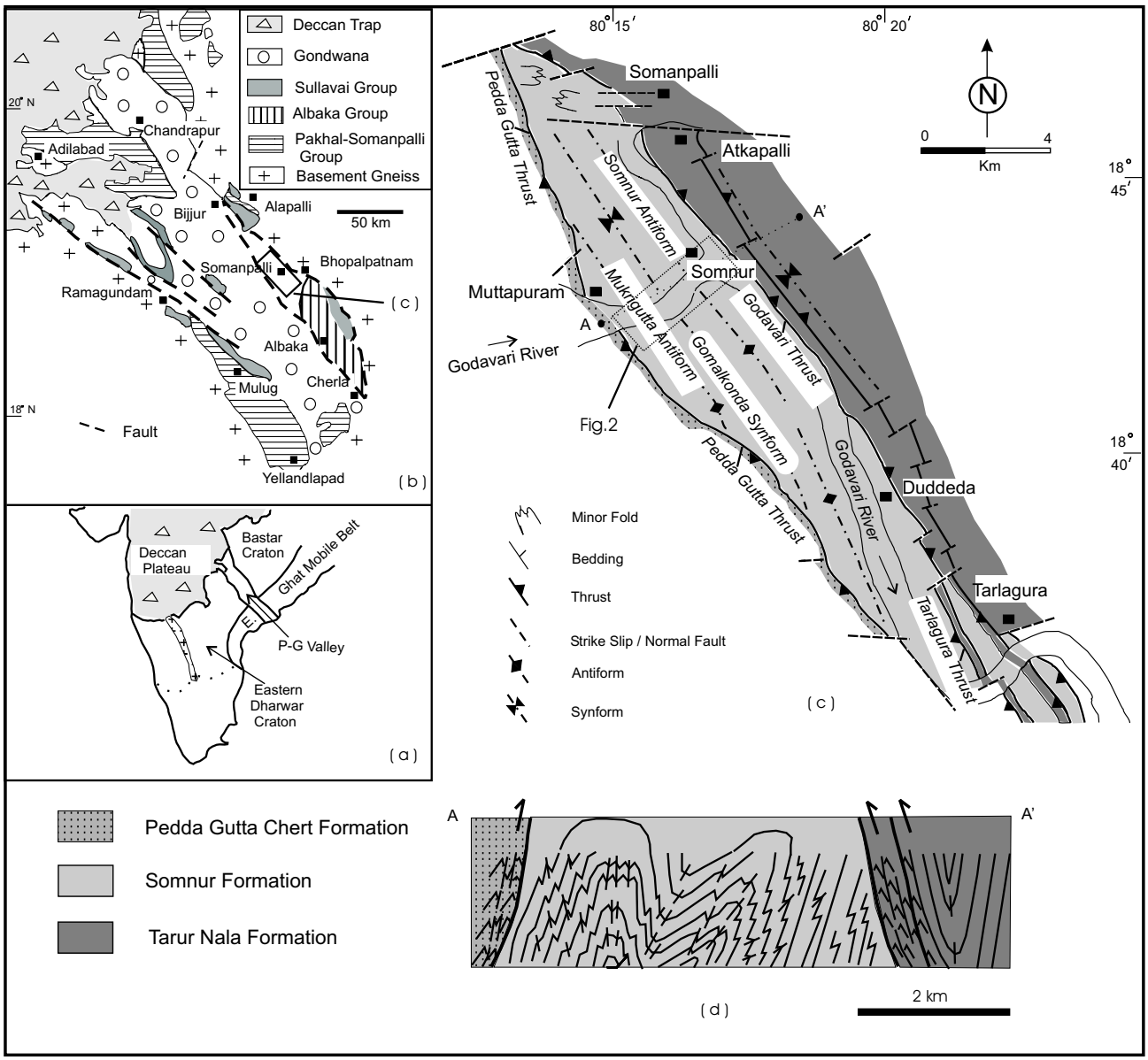

Figure 1. Geological map of the area around Somnur, eastern Proterozoic belt, Pranhita–Godavari (P–G) valley. Inset **(a)** the P–G valley basin along the join between the east Dharwar craton and the Bastar craton. **(b)** The major stratigraphic units in the P–G valley with actual position of the mapped area is shown in a rectangle. **(c)** Map showing major fold-and-thrust structures in the study area. **(d)** Structure section along tie line A-A′.

1992; Poblet and McClay 1996; Anastisio *et al* 1997; Suppe *et al* 1997). Development of asymmetric buckles has been a subject matter of several studies (Ghosh 1966; Price 1967; Price and Cosgrove 1990, p. 324–329). Minor asymmetric buckle folds develop readily at limbs of large folds due to shear modification of early symmetric buckles during flexural slip (Ramberg 1964). Development of asymmetric buckles has been successfully modeled by Ghosh (1966) by a combination of homogenous shortening and layer parallel shearing, the major contention being modification of early formed symmetric folds by later shearing. Alternatively, an obliquity between maximum compressive stress and layering may lead to asymmetric folds (Price 1967; Price and Cosgrove 1990).

A folded and faulted sedimentary succession belonging to the Mesoproterozoic Somanpalli Group (table 1; Ghosh 1997) occurs in a 30-km long fold-and-thrust belt along the eastern margin of the NW–SE trending Pranhita–Godavari (P–G valley) basin in south India (figure 1). These contractional structures occur along the join of the Bastar craton and the eastern Dharwar craton (Naqvi and Rogers 1987; Chaudhuri *et al* 2002). The Somnur Formation belonging to the Somanpalli Group is exposed

Table 1. *Lithostratigraphic succession of the Proterozoic Somanpalli Group around Godavari–Indravati confluence.*

Stratigraphic unit		Lithology	Broad depositional environment
Gondwana Supergroup	Chikiala Formation	Conglomerate, sandstone	Fluvial
— Fault —	— Fault —		
	Po-Gutta Formation (155 m)	Quartzose sandstone with minor pebble beds and sandstone-shale intercalations	Shallow marine
	— Unconformity —		
	Kopela Shale Formation (450 m)	Shale, interbedded sandstone-shale (minor)	Deep to shallow marine
	Pedda Gutta Chert Formation (250 m)	Chert-shale	Deep marine (?)
SOMANPALLI GROUP	Tarur Nala Formation (1250 m)	Chert-black shale, graywacke, limestone, ash beds, minor volcanics and litharenite	Starved, stagnated deep marine basin with turbidites
	Somnur Formation (1100 m)	Dominantly sandstone-shale with minor limestone and calcareous shale	Subtidal to supratidal
	Bodela Vagu Formation (220 m)	Limestone, marl, shale with minor sandstone, conglomerate and breccia	Intertidal to supratidal
	— Fault —		
	Basement Gneiss		

between two oppositely verging thrust sheets of the Tarur Nala Formation and the Pedda Gutta Chert Formation. Bounded between these two oppositely verging thrust sheets, asymmetric folds and other smaller brittle–ductile structures are recorded in the Somnur Formation (Ghosh 1997; Ghosh and Saha 1999; Ghosh and Saha 2003). The structures offer a unique opportunity to understand the kinematic development of large asymmetric folds in a fold-and-thrust belt. The evolution of Somnur fold-fault structures is dealt with by taking into consideration the geometry and overprinting relationship of mesoscopic structures and their relationship to larger structures. Spatial distribution of fold-fault structures, their geometry and kinematic indicators and finite strain data have been analysed to address issues related with development of the large asymmetric folds and associated structures within the Somnur Formation.

2. Geological setting

Proterozoic sedimentary successions in peninsular India occur in a number of cratonic basins formed after the amalgamation of some Archean nuclei in south and eastern India. One such important basin in the Pranhita–Godavari valley (P–G valley) occurs along the join of the east Dharwar and the Bastar cratons (figure 1a). The Proterozoic rocks of the P–G valley basin occur along two NW–SE trending belts separated by a central outcrop of Gondwana rocks and flanked on both sides by Archaean basement gneisses (figure 1b). The Somanpalli Group (Chaudhuri and Chanda 1991; Ghosh 1997; Saha and Ghosh 1998) in the northern part of the eastern Proterozoic belt is bounded on either side by faults (figure 1b). Basement gneisses of the Bhopalpatnam area (Bastar craton) occur in the east while the Gondwana rocks occur to the west. The Albaka Group of rocks overlies the Somanpalli sequence towards south. The gneisses of the Bastar craton lie along a faulted contact against the Proterozoic sedimentary sequences of the Somanpalli Group and the Albaka Group.

In the study area, around the confluence of Godavari and Indravati rivers, the deformed rocks (table 1) of the Somanpalli Group consist of several formations. The Somnur Formation (SF) crops out as a NW–SE trending belt between the Tarur Nala Formation (TNF) in the east and Pedda Gutta Chert Formation (PGCF) in the west and extends for a strike length of about 25–30 km (figure 1c). Tectonic dislocations, which are steep at current erosion level, separate strikingly dissimilar lithofacies associations within the Somanpalli Group. The deep marine turbidites of the TNF are thrust over the tidal–inter tidal sequence of the SF along an easterly dipping thrust named as the Godavari thrust. The rocks of the PGCF on the other hand is emplaced over the rocks of the SF from south–west

along a westerly dipping thrust, the Pedda Gutta thrust (Ghosh and Saha 2003; figure 1c and d).

Five members have been identified within the SF. These are, in ascending order, the Gangaram Shale member, the Tarlagura Quartzite member, the Gomalkonda Sandstone-Shale member, the Sangam Quartzite member, and the Duddeda Limestone member deposited in a tidal flat to shallow coastal environment (Ghosh 1997; Saha and Ghosh 1998). The TNF comprises deeper water chert, limestone-shale, graywacke and minor pyroclastics while the PGCF comprises only of chert and argillites (Ghosh 1997; Saha and Ghosh 1998). The calcareous to cherty argillites and cherts were deposited below the wave base with a limited contribution from terrigenous clastics. The juxtaposition of stratigraphic units with marked differences in depositional environments and rapid sedimentary facies changes have been interpreted as being due to extensional stage normal faults which ultimately controlled the formational boundaries (Saha 1992b; Ghosh 1997). Movement on a set of west dipping listric faults led to asymmetric half grabens which acted as repository for the Proterozoic sequences adjoining the Bastar craton.

Reactivation of extensional stage normal faults and moulding of folds against these faults occurred during later shortening of the basin across the basin strike (Saha 1990, 1992a; Ghosh 1997). The deformed rocks of the SF present large asymmetric folds and other mesoscopic brittle–ductile structures. In contrast the TNF and PGCF present highly cleaved rocks with transposition of bedding laminae and dismembering of fold trains by thrusts (Ghosh 1997; Ghosh and Saha 2003).

The dominant mineral paragenesis in argillaceous rocks of the Somanpalli Group is chlorite-white mica-quartz-opaque, a low greenschist facies assemblage indicating an ambient temperature of 300°C (Saha 1992b; Ghosh 1997). The bulk of the gneisses of the adjoining Bastar craton showing an assemblage of amphibole-garnet-plagioclase/quartz or brown biotite-garnet-plagioclase in the mafic bands indicates upper greenschist to amphibolite facies temperatures. Relict assemblages of orthopyroxene-clinopyroxene-garnet, preserved within the gneisses indicate low granulite facies protoliths (Saha 1992b).

3. Main folds

The quartzite members within the SF act as marker horizons in tracing the large scale asymmetric folds. Three such large folds – the Mukrigutta antiform (anticline) in the west, the Gomalkonda synform (syncline) in the middle and the Somnur antiform (anticline) in the east control the outcrop pattern of the SF (figure 1c). Axes of these major folds plunge gently either towards NW or SE. The axial traces of these major folds get truncated against the Pedda Gutta thrust, as well as the large E–W trending transverse fault in the northern part of the map area (figure 1c). In addition, smaller thrusts have developed within the SF marking domains with many inclined, asymmetric, tight, overturned mesoscopic folds, minor reverse faults and crenulation cleavage. Such domains of intense mesoscopic fold-fault development and shearing are termed here as fold-fault zones (FFZ). The FFZs occurring on two sides of the large antiforms (figure 2) have oppositely dipping cleavages and axial planes of small folds. Four FFZs have been recognized on the flanks of the Mukrigutta antiform and the Somnur antiform. These are named as the Mukrigutta Western FFZ (MWFFZ), the Mukrigutta Eastern FFZ (MEFFZ), Somnur Western FFZ (SWFFZ), and the Somnur Eastern FFZ (SEFFZ; figure 2).

4. Evolutionary sequence of structures

In order to work out the deformational history, the overprinting relationship of mesoscopic structures and their distribution within the domain of individual large structures has been analyzed. The geometry and orientations of minor folds and cleavage are generally consistent with the NW–SE trending large fold structures. The structures appear to have formed in a progressive three-stage sequence (Ghosh 1997; Ghosh and Saha 2003) – early buckle folding and cleavage development followed by thrusting and development of FFZs and finally conjugate strike-slip faulting as outlined below.

4.1 *Folding and cleavage development*

The marked competency contrast between quartzite and shale units or limestone and shale units within different lithological units of the SF favoured early initiation of buckles dominating over layer parallel shortening. The minor second and third order folds are congruous to the mapped large antiforms and synforms, designated as first order folds. Two sets of minor folds are observed in the Somnur transect (figure 2). The shapes of mesoscopic folds set-1 change from upright and near symmetrical in hinge areas (figure 3a) to inclined and asymmetrical in limbs (figure 3b) of the first order folds. Folding was accompanied by the development of a pervasive cleavage roughly

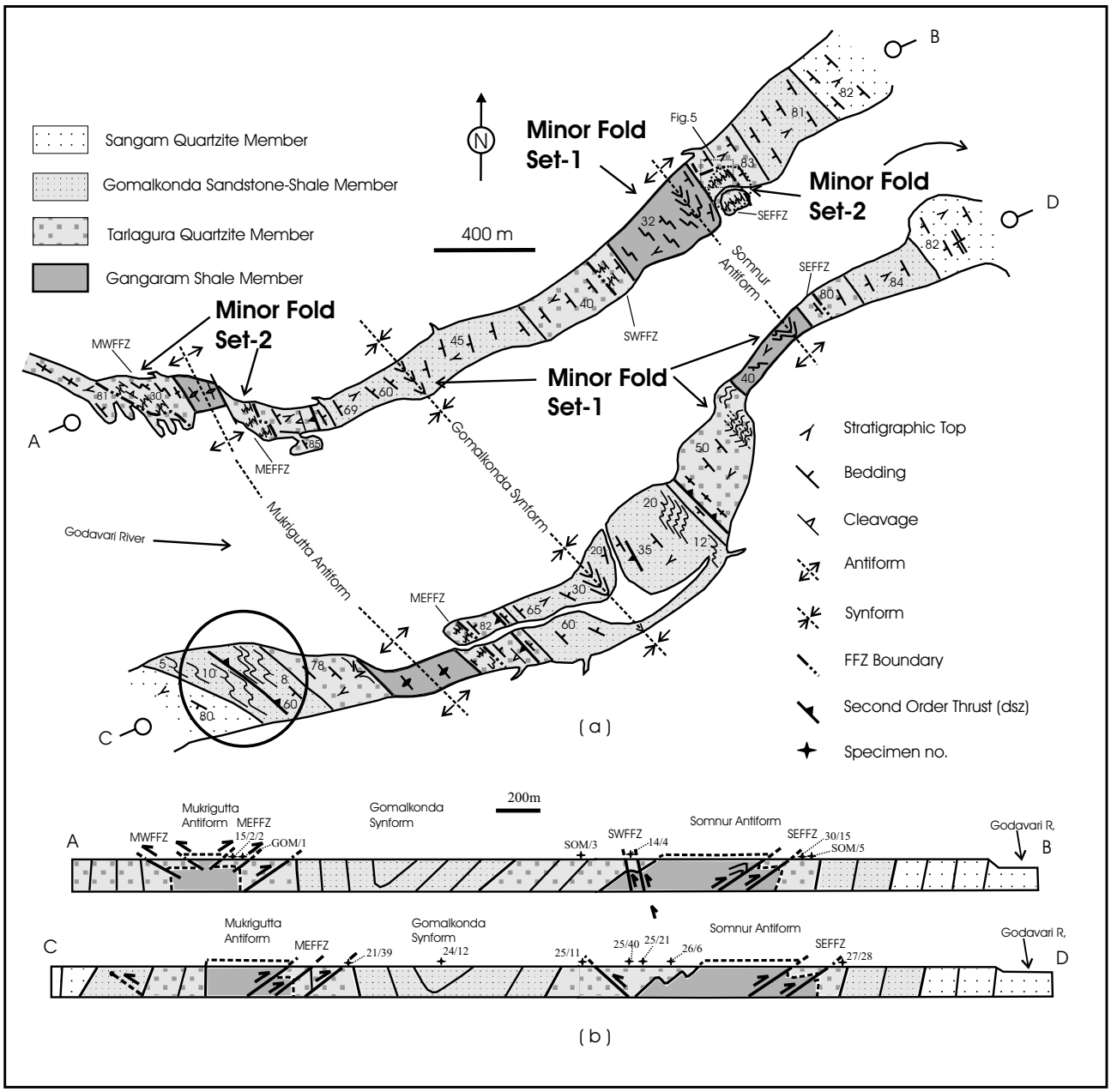

Figure 2. **(a)** Strip maps showing disposition of the lithostratigraphic units and different orders of structural features within the Somnur Formation along the two banks of Godavari River. For location see figure 1(c). **(b)** Structural sections drawn along the north and south banks of river Godavari. Numbered locations correspond to samples for strain analysis (tables 2 and 3).

parallel to the axial plane of mesoscopic folds (figure 3c) with a weak cleavage fanning. The orientation of fold axes is more or less constant in a small outcrop, but regional variation from gentle northwesterly plunge to southeasterly plunge is observed (figure 4a–c). The orientation of axes and geometry of these mesoscopic folds (minor fold set-1) is congruous with that of the large folds (figure 4a–c).

In general the cleavage strikes NW–SE and is vertical to steep southwesterly dipping (figure 4a–c). Bedding-cleavage angle in fold limbs is 50°–60° in competent quartzite and limestone layers. It decreases to 20° or less in incompetent shale or calcareous shale horizons. A lithologically controlled cleavage refraction pattern is evident. Quartz veins parallel to or at low angles to cleavage planes show boudinage while those at higher angles to cleavage show folds. The axial planar nature of cleavage with weak fanning implies that cleavage development was broadly contemporaneous with the major folds.

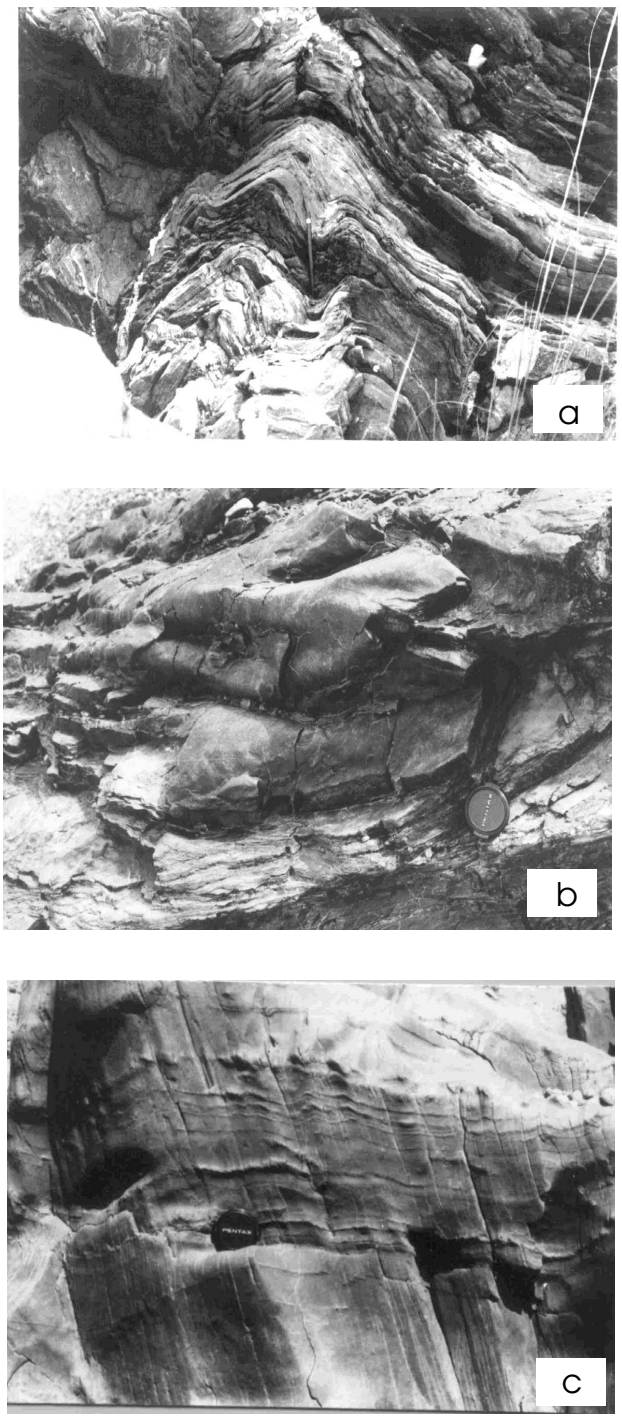

Figure 3. **(a)** Upright near symmetric minor folds, Tarlagura Quartzite Member, view looking north; **(b)** Asymmetric minor folds, Tarlagura Quartzite Member with fold axes plunging gently towards NW or SE, view looking north; **(c)** Steep south–westerly dipping axial-planar cleavage developed at large antiformal hinge, vertical section, looking towards south.

Other common features on limbs of mesoscopic folds are flexural slip induced quartz slickencrysts sub-perpendicular to fold hinges and arrays of en-echelon, quartz filled tension gashes. On joint faces perpendicular to fold axis individual tension gashes tend to form at 45° or lesser angle to bedding and take sygmoidal form at places. The geometry of the tension gashes indicate local top-towards-antiformal hinge bedding parallel shear, which is compatible with shear sense indicated by quartz slickenside steps (Twiss and Moore 1992, p. 61).

The alternate quartzitic and shaly (slaty) members of the SF provided an ideal setting for folding by buckling of multilayers with competent quartzite horizons acting as the control units (Price and Cosgrove 1990). The sense of movements deduced from quartz filled tension gashes and quartz slickencrysts on limbs of large folds, are consistent with a top-towards-antiformal hinge shear indicating their formation through secondary effects of flexural slip on the limbs of the large folds. The overall axial planar nature of regional slaty cleavage, weak cleavage fanning and refraction of cleavage in alternate competent and incompetent layers, indicate that flexural slip mechanism worked in combination with layer parallel homogeneous shortening (Donath and Parker 1974).

4.2 *Thrusts and conjugate FFZs*

A stage of thrusting and FFZ formation followed early flexural slip folding and cleavage formation. The NW–SE striking and oppositely dipping (either towards NE or SW at 40°–45°) FFZs have developed in conjugate sets across the large folds in the map area (figure 2b). Internally the FFZs are characterized by inclined, asymmetric, tight, overturned folds, reverse faults and inclined cleavage (figure 5). A second set of minor folds (set-2) incongruous to the large folds occurs in the FFZs. The asymmetry of the set-2 minor folds is consistent with the sense of slip deduced from slickensides on minor faults and shear bands within the FFZs, indicating linked development of fold set-2 and FFZs. These are southwesterly verging asymmetric S folds and northeasterly verging asymmetric Z folds at MWFFZ and MEFFZ respectively (figure 6a). SWFFZ and SEFFZ show similar variation in the geometry of mesoscopic folds (set-2) across the Somnur antiform. These minor folds are labelled as minor fold set-2 to distinguish them from congruous minor folds (set-1) reported from domains on the limbs of the Mukrigutta or Somnur antiforms (section 4.1), which are not affected by FFZ's. Contrary to set-2 minor folds, congruous minor folds (set-1) have asymmetric Z and S shapes respectively on the western limb and eastern limb of the Somnur antiform.

These minor folds (set-2) from the FFZs are noncylindrical with slightly curved hinges. Orientations of fold axes define a girdle coinciding with

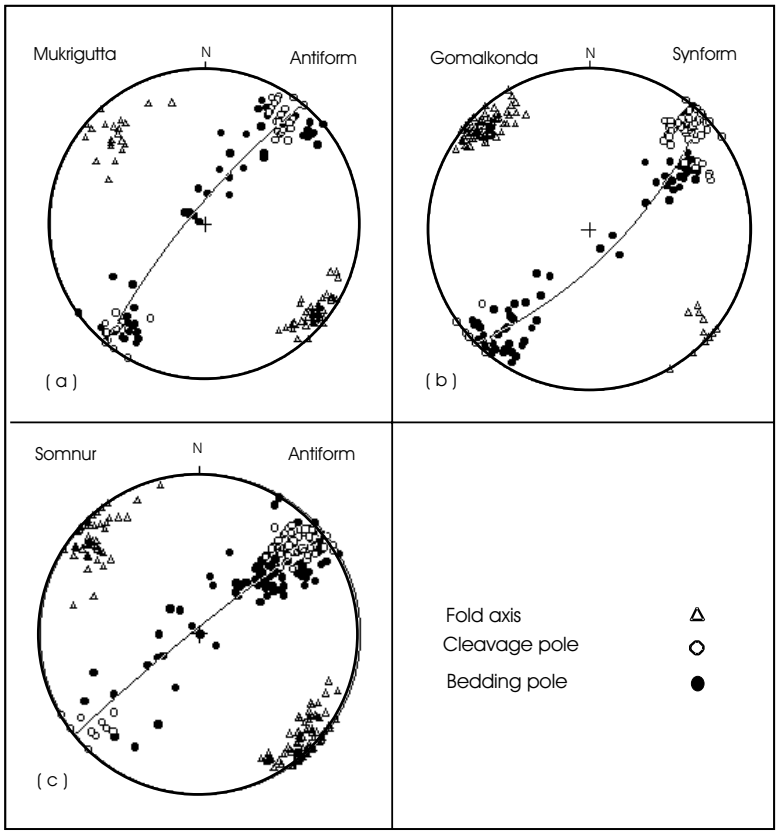

Figure 4. Orientation of different structural elements from the Somnur Formation. **(a)** 62 bedding poles, 40 cleavage poles and 63 fold axes, Mukrigutta antiform; **(b)** 76 bedding poles, 67 cleavage poles and 80 fold axes, Gomalkonda synform; **(c)** 117 bedding poles, 61 cleavage poles and 120 fold axes, Somnur antiform.

the average orientation of associated reverse faults and crenulation cleavages (figure 7a–b). In outcrop scale mesoscopic folds get displaced by minor reverse faults at their steeper limbs (figure 8a). Slickensides on faults (figure 8b), fold asymmetry, orientation of stretching lineation, minor fault offsets and shear band cleavages were used to decipher the sense of slip within FFZs. For example, the sense of slip is top-to-southwest in MWFFZ but top-to-northeast in MEFFZ (figure 2). Shear band cleavage locally present within the FFZs transposes (Turner and Weiss 1963) the main axial plane cleavage (S_1; figure 8c). The reorientation of S_1 and its transposition within the FFZ suggest that the FFZs evolved at a late stage after major shortening was accommodated by the major folds and slaty cleavage development. Apart from FFZs, the second order thrusts were also produced at this stage. Train of set-1 minor folds, congruous with major folds are displaced/disrupted by second order thrusts such as in the domain of western limb of the Mukrigutta antiform on the southern bank of Godavari river (see figure 2a, circled area). These are both southwesterly and northeasterly dipping (figure 2). Deformation in the vicinity of these faults is expressed by zones of highly sheared rocks a few meters thick, marked by intense fracturing and quartz veining.

4.3 *Conjugate strike-slip faulting*

The third recognized structural stage is an episode of conjugate strike-slip faulting developed in both mesoscopic and large scale. A NNE–SSW set with dextral and an E–W set with sinistral sense of movements apparently form a conjugate pair (figure 9). The regional compression direction as deduced from these conjugate strike-slip faults lie in the NE–SW quadrant consistent with the shortening associated with major fold-and-thrust structures (figure 9). Late mesoscopic strike slip faults (figure 10a) and brittle shear zones (figure 10b) cut across regional cleavage, minor folds and faults. The axial traces of first-order folds get truncated against E–W faults in the northern part of the map area (figure 1c).

5. Finite strain and its variation across the belt

Two dimensional strain was estimated from each of the two mutually perpendicular thin sections cut

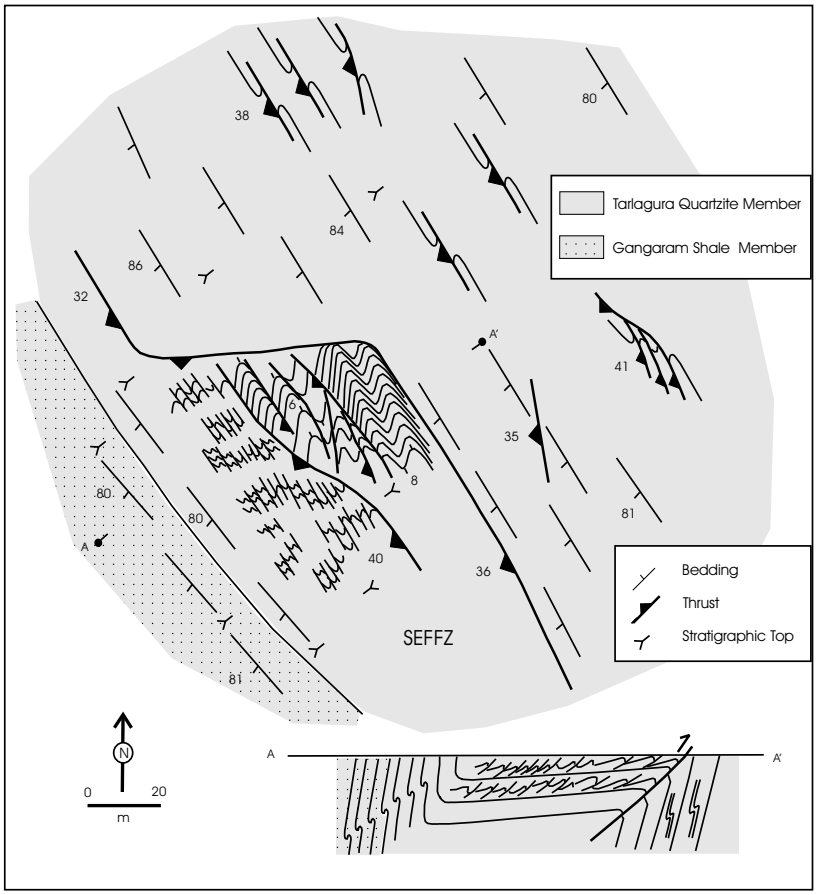

Figure 5. Fault arrays and small folds in the Somnur EFFZ. Structure section (bottom) is along tie line AA′. Location in figure 2.

from oriented quartzite specimens from the Somnur Formation (numbered locations in figure 2b). One of the thin sections was cut sub-parallel to stretching lineation and perpendicular to foliation (XZ section) while the other was cut sub-parallel to fold axis and perpendicular to foliation in the specimen (YZ section). The reference directions were defined by foliation traces on these sections. The long and short directions of the 'clasts' were measured in an optical microscope using a micrometer ocular. Fluctuation of the long axis from the reference direction was obtained from the amount of stage rotation necessary to bring the long axis parallel to reference direction. The 'clasts' are single grains of quartz that have undergone various degrees of dynamic recrystallization leading to alteration in the shapes of the clasts which introduce a bias in measurement particularly at a high matrix-clast ratio. For this reason, outline of the thoroughly recrystallized clasts were measured in plane-polarized light where grain boundaries are recognized through concentration of phyllosilicates along them (figure 10c). Final two dimensional strain ratios (R_s values) were obtained from the measured values of R_f and φ (Ramsay 1967; Dunnet 1969) in each thin section using the hyperbolic net of De Paor (1988). The strain values thus obtained were cross-checked using an algebraic method of Robin (1977). The magnitudes of strain determined by the two methods do not differ by more than 5%, on an average, for the measured samples (Ghosh 1997; Ghosh and Saha 2003). Orientations of the principal strains from the two methods are within a few degrees of each other. Three-dimensional strain was calculated (table 2) from the two dimensional strain ratios assuming constant volume deformation.

The shapes of strain ellipsoids thus obtained are shown in a conventional Hsu plot (figure 11a). Estimates for different strain parameters are summarized in table 2. The finite strain ellipsoids fall in the apparent flattening field. Although finite strain is of the flattening type in all measured specimens, a systematic variation in strain magnitude and orientation is noticeable (figure 11b). The strain values are relatively higher at large scale fold hinges (R_{XZ}: 4.8) such as at the hinge of the Gomalkonda synform (figure 11b) and at steep overturned limbs (R_{XZ}: 3.6–4.0) of the Mukrigutta and Somnur antiforms (figure 11b) in

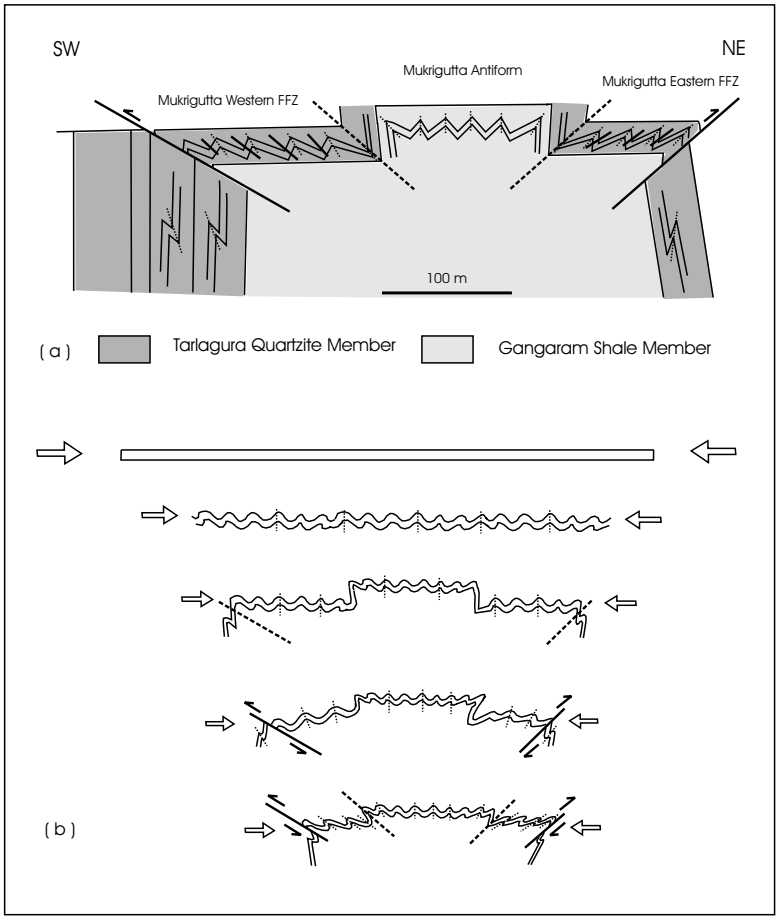

Figure 6. **(a)** Fold-fault zones affecting the Mukrigutta antiform. The asymmetry of minor folds changes from north–easterly verging in the EFFZ to south–westerly verging in the WFFZ. **(b)** Model (not to scale) illustrating development of oppositely dipping FFZs (see text for detail).

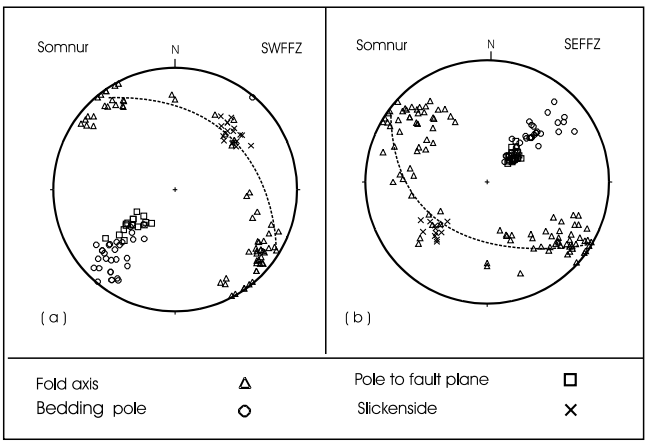

Figure 7. Orientation of different structural elements from the Somnur Formation. **(a)** 60 fold axes, 31 cleavage poles, 17 poles to minor faults and 17 slickensides, Somnur western fold-fault zone, note spread in fold axes orientation; **(b)** 91 fold axes, 33 cleavage poles, 24 poles to minor faults and 12 slickensides, Somnur eastern fold-fault zone.

comparison to the right way up, moderately dipping limb (R_{XZ}: 3.1–3.7) of the Somnur antiform (figure 11b). The highest strain value is obtained from second order thrusts or FFZs (R_{XZ}: 3.9–7.3) irrespective of whether these develop at overturned or steep limbs, at hinges or at moderately dipping limbs of the Mukrigutta and Somnur antiforms (figure 11b; table 3).

5.1 *Strain factorization*

Distributed shearing within the FFZs is apparent from changes in cleavage orientation, inclined asymmetric folds, wide variation in fold axes orientation and common occurrence of minor faults. To test whether the values of shear strain (γ) is actually higher in these zones; measured finite strain data are factorized into stretching (λ) and shear (γ) components.

In strain factorization, a sequence of strain superposition must be assumed. As established from the superposition of mesoscopic fabrics a sequence of pure shear shortening followed by simple shear has been chosen in the present case. Following the analysis of strain in thrust sheets (Sanderson 1982), which undergo components of

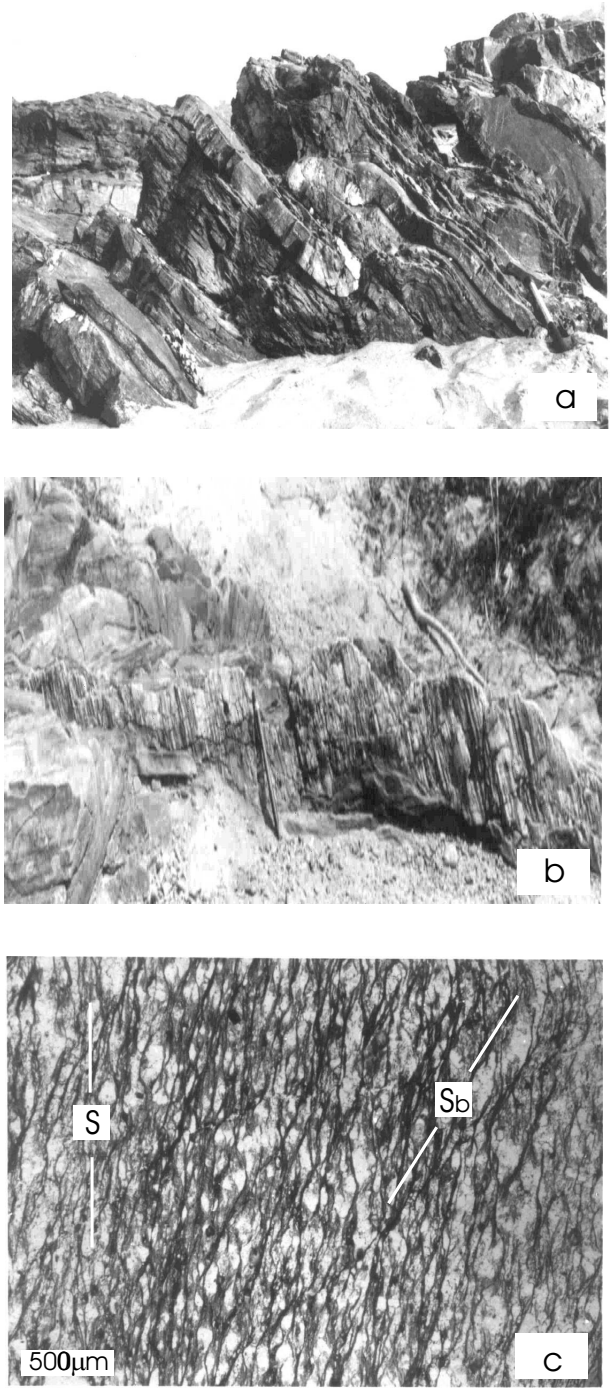

Figure 8. **(a)** Minor thrust dipping south–west displace short, overturned limbs of north–easterly verging asymmetric folds at SEFFZ; **(b)** Quartz slickencrysts on minor reverse faults cutting subhorizontal beds at MWFFZ; **(c)** photomicrograph showing shear-band cleavage (S_b) transposing steep regional disjunctive cleavage (S), SWFFZ.

pure shear in the direction of thrust transport and simple shear, Saha (1989) considered how an axial plane cleavage related shortening strain ($k < 1$) is modified by superimposed simple shear within a break thrust. In this analysis it is also assumed that

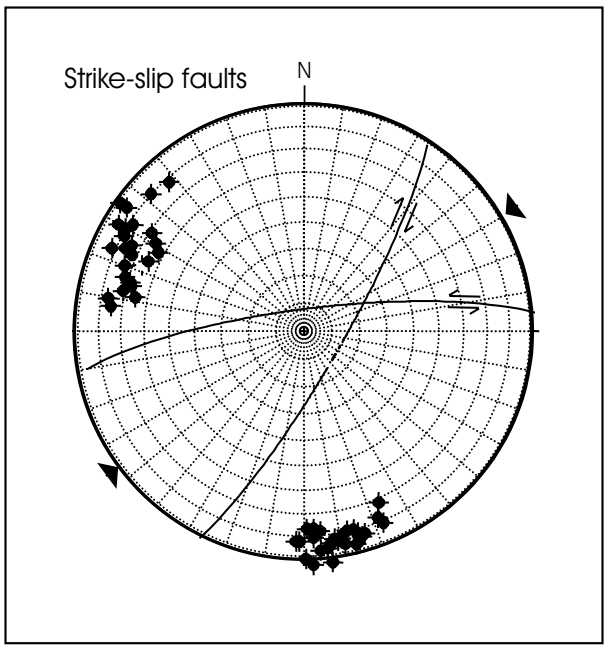

Figure 9. Orientation of conjugate sets ($n = 49$) of minor strike-slip faults from the Somnur Formation indicating NE–SW maximum principal compression direction (arrow head; after figure 10(a) of Ghosh and Saha (2003)).

λ_2 (or Y) associated with the axial plane related cleavage strain is parallel to Y associated with superimposed simple shear as the gross orientation of axial traces of large fold and trends of FFZs match closely. Strain values are plotted in a modified Flinn diagram (figure 11c; Saha 1989). Factorization of strain gives an estimate of γ between 0.75 and 3, the lower values such as $1 < \gamma < 0.5$ in specimens 25/21 and 25/11 are coming from outside the FFZs whereas higher values such as $\gamma > 2$ as in specimens 15/2/2 and GOM/1 are coming from within the FFZs (figures 2b and 11b).

The simple shear component γ can also be determined by rewriting Sanderson's (1982) equations (7a) and (7b) to solve for γ (Evans and Dunne 1991).

$$\gamma = (R^2 - 1)/(\text{Cot } \theta + R^2 \tan\ \theta),$$

where R is the strain ratio and θ is the angle between the long axis λ_1 and shear zone boundary. The major folds in Somnur Formation rocks are of the same trend as that of the FFZs (e.g., MWFFZ). Considering the average dip of minor fault populations within the FFZs as well as from enveloping surfaces of inclined folds, the shear zone walls are assumed to dip at 40–45° either northeasterly or southwesterly. On a cross section perpendicular to the major fold trend (figure 2a and b), the FFZ boundary as well as the dip line of the array of mesoscopic faults is on an average at a very low

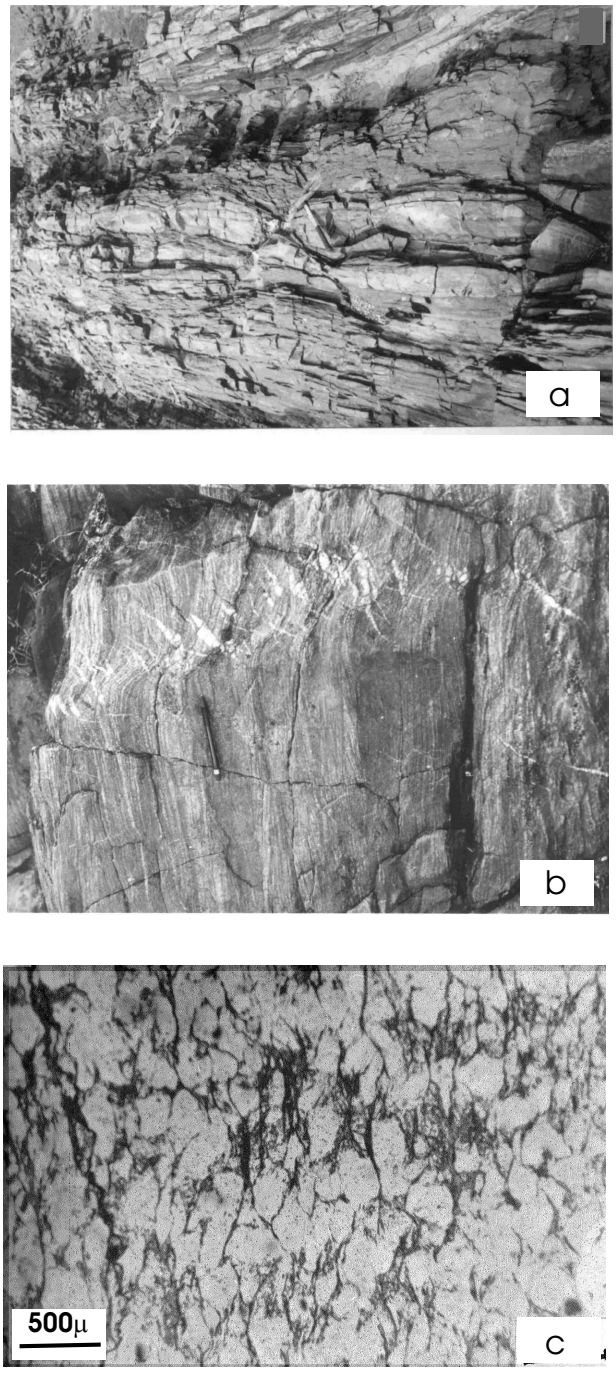

Figure 10. **(a)** Conjugate strike-slip faults, steep eastern limb of the Somnur antiform, plan view, bedding trace (left to right on photo) trends NW–SE; **(b)** Semi-brittle shears within quartzite, plan view, bedding traces trend NW–SE, tension gashes indicate dextral strike-slip movement at high angle to bedding; **(c)** Thin section of a quartzite rock from Somnur Formation showing deformed quartz clasts in plane polarized light which were used in strain analysis.

angle ($< 10°$) with the axial plane cleavage trace. θ as defined here is the angle between axial plane of minor folds (axial plane cleavage) and minor faults in FFZs (or shear band cleavage) as measured on cross section. As the observed angle between axial planes of inclined folds and associated minor faults or that between axial planar cleavage and shear band structures is usually very low (5–10°), we assume $\theta = 5$–$10°$. The computed values of γ range between 1 and 3.5.

Linear features such as fold hinges are shown to rotate towards the transport direction in zones undergoing simple shear (e.g., Escher and Watterson 1974; Mawer and Williams 1991). The degree of fold axis rotation places a constraint on shear zone orientation and maximum shear strain value (Skjernaa 1980). Fold hinges within the FFZs only show minor reorientations within the axial surface. In Skjernaa's (1980) mathematical model, significant rotation of fold axes towards stretching direction occurs at $\gamma = 3$. Thus all the three approaches indicate $\gamma \approx 3$ as a maximum value of shear strain in these zones.

Measurement and partitioning of strain data above shows that a definite strain gradient occurs in the area in the form of FFZs where both γ and λ values are greater in comparison to other parts. However, bulk finite strain is of the flattening type. The flattening type ellipsoids within FFZs are apparently a result of flattening (pure shear) followed by shearing (Sanderson 1982; Saha 1989). This seems to be a valid interpretation in the light of the observed mesoscopic structures, namely the presence of an axial planar cleavage, the array of minor faults and shear bands cutting the reoriented axial planar cleavage in FFZs.

6. Discussion

6.1 *The FFZs: their extents and variation in strain*

A variation in finite strain data exists across the Somnur transect with highest values being observed from within the FFZs (figure 11b). The noncylindricity of minor folds (set-2), preferential distribution of fold axes in a girdle, rotation of S_1 cleavage and its transposition by a shear band cleavage within FFZs can be best explained in terms of a distributed shearing within the FFZs. The strain partitioning data also clearly show that there is a definite increase in noncoaxiality expressed in terms of increase in γ value as one approaches the FFZs ($\gamma = 3$) from domains of large folds ($\gamma = 0.75$; figure 11c). The observed variation in geometry and orientation of mesoscopic folds (set-2) in FFZs, in comparison to the folds (set-1) in limbs and hinges of large folds are interpreted to form as a result of this increased shearing within the FFZs (figure 6b).

Table 2. *3-D strain ratios, shape of strain ellipsoids (ν and κ) and strain intensity (ε_s) calculated from quartzites of the Somnur Formation (T^t = total strain).*

Specimen no.	$T^t(R_f/\phi)$	κ	ν	ε_s
21/39	3.94 : 2.78 : 1	0.24	0.48	0.99
24/12	4.86 : 3.45 : 1	0.17	0.56	1.18
25/11	3.92 : 2.63 : 1	0.31	0.41	0.98
25/40	3.46 : 2.44 : 1	0.29	0.44	0.91
25/21	3.10 : 2.22 : 1	0.32	0.41	0.82
26/6	3.74 : 2.63 : 1	0.26	0.46	0.96
27/28	3.97 : 2.63 : 1	0.32	0.39	0.99
30/15	3.73 : 2.70 : 1	0.21	0.53	0.95
15/2/2	7.36 : 4.00 : 1	0.27	0.39	1.46
GOM/1	6.00 : 3.70 : 1	0.23	0.46	1.30
SOM/3	3.75 : 3.50 : 1	0.23	0.50	0.96
14/4	4.84 : 3.12 : 1	0.26	0.44	1.16
SOM/5	3.56 : 2.44 : 1	0.32	0.41	0.92

$$\kappa = \frac{(\lambda_1/\lambda_2)^{1/2} - 1}{(\lambda_2/\lambda_3)^{1/2} - 1}; \quad \nu = \frac{2\varepsilon_2 - \varepsilon_1 - \varepsilon_3}{\varepsilon_1 - \varepsilon_3}$$

$$\varepsilon_s = \frac{1}{\sqrt{3}}\sqrt{(\varepsilon_1 - \varepsilon_2)^2 + (\varepsilon_2 - \varepsilon_3)^2 + (\varepsilon_3 - \varepsilon_1)^2}$$

The geometry of large folds in profile gets modified wherever they are associated with FFZs. The Mukrigutta antiform or the Somnur antiform attain the shape of asymmetric box folds near the northern bank of Godavari river with wide hinge, western moderately dipping back limb and eastern steep to overturned fore limb, due to development of two oppositely dipping FFZs (figure 2b). However the same folds in the southern bank appear as simple asymmetric folds as the easterly dipping FFZs die out (figure 2b). Thus the FFZs are considered to have formed later than the large antiformal structures, Mukrigutta antiform or Somnur antiform, whose geometry is modified by the FFZs (figure 6a).

The FFZs have much smaller geographic extent in comparison to the large folds. While major fold axial traces run for at least 15–20 km in the map area, the strike extent of FFZs and second order thrusts are limited (1–2 km; figures 1c and 2). That along strike continuity of the FFZs is limited, is well demonstrated from a comparison of the strip maps for the north and southern banks of river Godavari around Somnur (figure 2a). The inclined minor folds of SWFFZ in north bank gives way to regular trains of congruous minor folds (set-1) in the western limb of the Somnur antiform. Evidently the SWFFZ ceases to continue along strike to the southern bank. Therefore the FFZs are interpreted as shallower structures with extension along depth not exceeding several tens of meters, in comparison to the large folds.

6.2 *Fixed hinge folds*

Development of finite amplitude folds may or may not involve hinge migration. In the case of fault bend folds of kink geometry, a section of the folded strata passes alternatively through limb and hinge domain, as the hanging wall strata is displaced from a lower flat through the ramp to a higher flat. Fabric typical of hinge region may thus be overprinted by those expected in the limb and *vice versa*. One of the geometric requirements of limb rotation around a pinned hinge is that flexural slip should be of opposite sense across the hinge and there is no overprinting of expected hinge fabric. Field data on geometry of folds and rock fabrics are usually utilized to differentiate fixed-hinge fault related folds from migrating-hinge folds (Fischer *et al* 1992; Fischer and Anastasio 1994; Homza and Wallace 1995; Zapata and Allmendinger 1996; Suppe *et al* 1997). Hedlund *et al* (1994) reported thrust related fixed hinge folding based on growth patterns of antitaxial fibrous overgrowths and veins. Stewert and Alvarez (1991) demonstrated that some folds in the Umbria Marche Apennines grew by the lateral migration of axial surfaces. Their contention is based on variation in sense of shearing of refracted cleavage and imbricates around some first-order thrust cored anticlines which is not always consistent with that predicted by flexural-slip towards a pinned hinge.

But unlike situations where mesoscopic fabrics are more abundant away from the hinges and shear

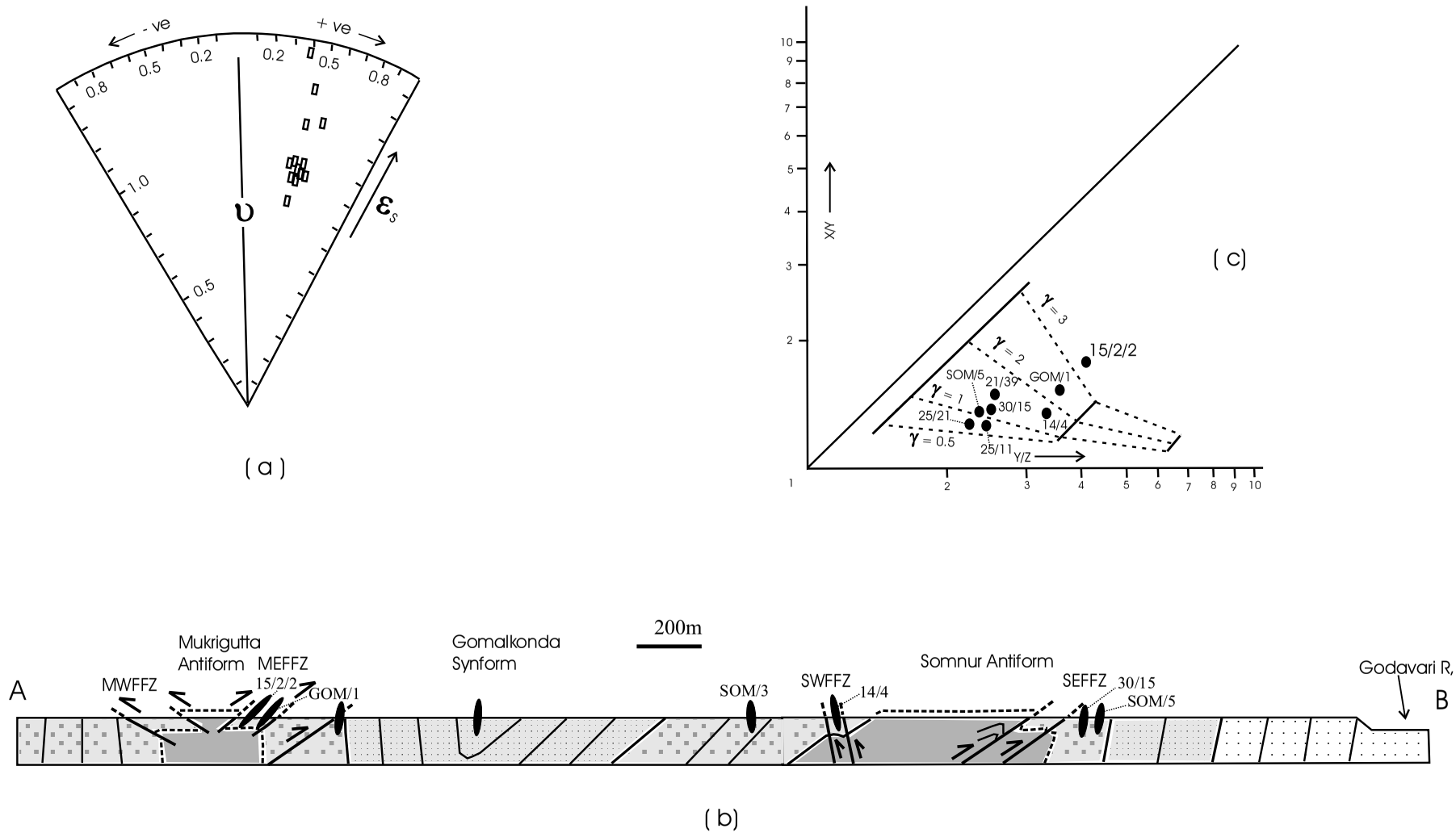

Figure 11. Shape of strain ellipsoids measured from quartzites of the Somnur Formation on **(a)** Hsu plot; **(b)** Structural section drawn across the Somnur transect showing 2-D strain ellipses (XZ) in different structural domains; **(c)** Plots of total strain on a modified Flinn plot (after Saha 1989) for estimation of shear strain from selected specimens of Somnur quartzite showing gradation in strain values. 'θ' indicate obliquity of the shear zone boundary with respect to pre-shearing X–Y plane.

Table 3. *Range of maximum strain ratio (X:Z) and shape of finite strain ellipsoid (k) in different structural domains from the Somnur Formation.*

Rock unit (strain gauge)	Structural domain	X:Z	k	Remarks
Somnur Formation (grain shape fabric)	Major fold hinge area	3.7–4.2	0.17	–
	Fold-fault zones	3.9–7.3	0.27–0.32	Non-coaxial deformation indicated by curved fibres in pressure shadows
	Moderately dipping limb	2.5–3.4	0.23	–
	Overturned limb	4.0	0.26–0.27	–

sense reversals occur in the forelimbs of major anticlines (e.g., Stewart and Alvarez 1991; Tavarnelli 1997), first order fold hinges in the Somnur transect are marked by abundant minor folds of set-1 and intense slaty cleavage. Reversal of shear sense as deduced from asymmetry of conguous minor folds or slickenside steps are disposed symmetrically with respect to the first order hinges. Mesoscopic structures typical of limbs of large folds, e.g., en echelon tension gashes, slickencrysts on bedding, do not overprint structures typical of hinges, e.g., subvertical cleavage and symmetric minor folds. First order folds around Somnur are thus interpreted as fixed hinge folds.

Variation of finite strain across the transect shows that the hinges and steep or overturned limbs of large fold present higher strain values (R_{XZ}: 3.6–4.8) in comparison to their moderately dipping limbs (R_{XZ}: 3.1–3.7). Flexural slip with layer parallel homogeneous shortening models successfully explain such occurrence of higher strain values at hinges and at more rotated limbs of folds (Twiss and Moore 1992, p. 240) than the other models like pure flexure, shear or flexural slip (Ramsay and Huber 1987, p. 457; Twiss and Moore 1992, p. 240). The accumulation of strain in fold hinges is a function of strain rate and tightness of those hinges. If the hinges remain fixed during progressive folding, strain accumulation will be more in such hinges compared to the limbs, but fold hinge migration is bound to leave evidence in terms of more uniform distribution of strain values or higher strains to occur at forelimbs and backlimbs, once the interlimb angle is reduced to ±140° or less (Fischer *et al* 1992; Fischer and Anastasio 1994). Thus observed strain data (higher values at hinges in comparison to limbs excepting the FFZs) together with distribution of mesoscopic structures further constraints fixed-hinge folding to be the viable mechanism of large scale fold development within the Somnur rocks.

6.3 *Modification of large folds by layer parallel shear – the development of asymmetry*

It is apparent from a study of minor folds in FFZs and adjacent large fold domains that early formed mesoscopic folds (set-1) were later modified within FFZs and formed a second set of minor folds (set-2). Asymmetry and vergence directions of minor folds (set-2) within FFZs is in striking contrast to what is expected of minor congruous folds (set-1) on the limbs of higher order folds. The presence of higher shear strain values in the FFZs indicate the influence of shearing in shape modification of set-1 folds to form tighter and oppositely inclined set-2 folds. Moreover the FFZs have modified the profile of large folds locally, but their geographic extents are too small to control the overall development of the regional asymmetric folds in Somnur rocks.

Asymmetric folds readily form when earlier symmetrical folds are subjected to simple shear parallel to the enveloping surface of the folds (Ghosh 1966). The earlier folds are tilted in one direction to a monoclinic symmetry. Asymmetric folds are also shown to form in experiments under combined simple shear and pure shear (Ghosh 1966). The combination of simple shear and pure shear brings the resultant strain ellipsoid in such a position that plane of maximum shearing strain becomes nearly parallel to the enveloping surface. Price (1967) noted that the axis of maximum compressive stress, prior and subsequent to fold initiation, can act at a significant angle to layering, as could be inferred from field evidence. He argued that in such situations the layer parallel shearing stresses and consequent bending moment could explain initiation of asymmetric buckles. However the presence of high fluid pressure (often displayed by profusion of crystal fibres) along bedding planes inhibit significant shear stresses to exist along such planes (Price and Cosgrove 1990, p. 328) hindering formation of large

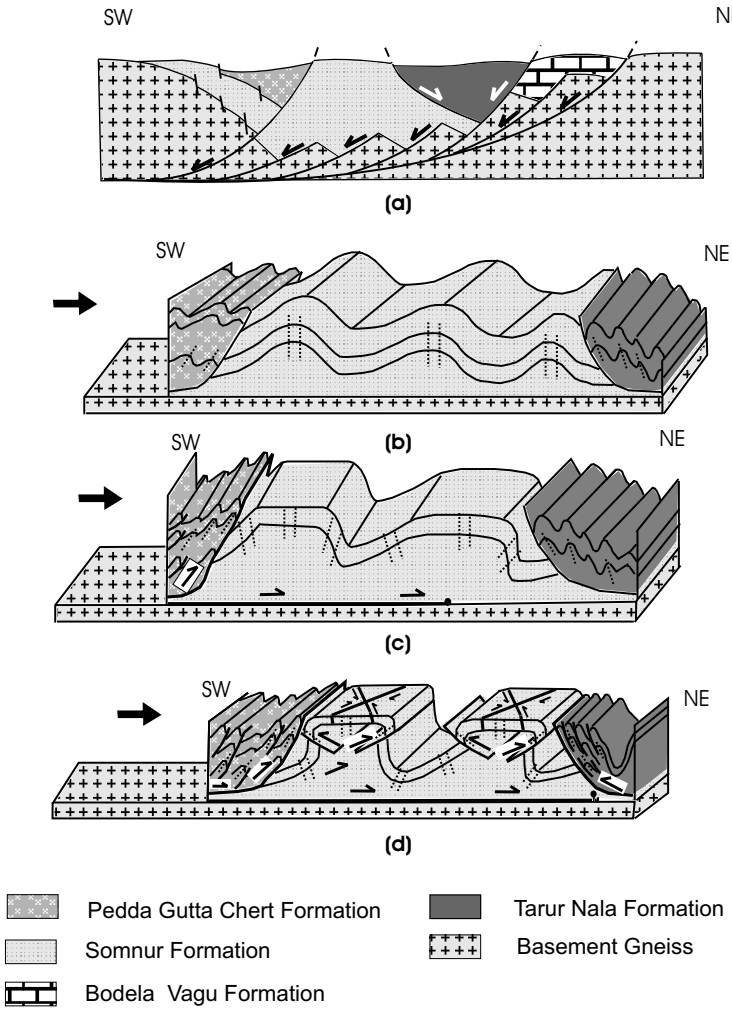

Figure 12. Schematic drawing to illustrate kinematic evolution (**a**–**d** in relative time sequence) of thrusts, folds and FFZs within the Somnur Formation and adjacent Pedda Gutta Chert Formation and Tarur Nala Formation of the Proterozoic Somanpalli Group.

asymmetric buckles by the mechanism invoked by Price (1967). Asymmetric buckle fold development thus requires a syn or later layer parallel shear which modifies the geometry of early formed symmetric upright buckles and brings about changes in symmetry and inclination of the folds (Ghosh 1966; Sanderson 1979). Thus to explain asymmetric folds within the SF, one may consider the presence of a layer parallel shear in conjunction with layer parallel shortening. Such large scale layer parallel shearing is possible if the layered sedimentary sequence (the Somanpalli Group) gets detached from the basement (the gneissic rocks of the Bastar craton) and moves over a basal decollement as the package gets shortened.

The gneissic basement rocks of the study area occur east of the exposure of the rocks of the Somanpalli Group and are separated from the latter by a steep fault. It does not get repeated within the Somanpalli Group barring any chance of it being thrusted up or folded within or along with the overlying supracrustals. A tell-tale difference in metamorphic grade exists across the supracrustal-gneissic contact with the upper greenschist to lower amphibolite facies of the latter indicating its higher depth of burial in comparison to the low greenschist facies assemblages of the overlying supracrustals of the Somanpalli Group. Recycling of early formed structure is possible in basins where an extensional regime is followed by a contractional regime and *vice versa* (Jackson 1980; Butler 1989; Williams *et al* 1989). Old fault zones are mechanically favoured for such renewed movements (Etheridge 1986; White *et al* 1986). The listric extensional stage normal fault marking the eastern boundary of the asymmetric half graben basin hosting the supracrustals of the Somanpalli Group (Saha 1992a and b) is an ideal candidate for such renewed movements at the onset of the later contractional deformation. Its reactivation as

a regional decollement and northeastward movement of supracrustals is considered sufficient to generate the layer parallel shear for modification of the geometries of the large folds.

Thus it is postulated that during NE–SW shortening, the sedimentary succession got detached from the basement along the master decollement (figure 12a) and was shortened dominantly through buckling and cleavage development (figure 12b). With continued shortening the extensional stage normal faults were reactivated as thrust faults. The PGCF was thrusted over the Somnur rocks from SW. In a forward breaking sequence, Somnur rocks also moved NEward along the basal decollement (figure 12c). On the contrary, the rocks of the TNF were thrusted over the Somnur rocks from SW, moving in an opposite direction. The SWward vergence of Tarur Nala rocks was primarily controlled by a pre-deformational steep NEasterly dipping fault, separating adjacent shallow and deep water sequences, which was later reactivated as a thrust fault during NE–SW contraction (Ghosh 1997; Ghosh and Saha 1999; Ghosh and Saha 2003). The Tarur Nala thrust sheet registered a buttressing effect on NEasterly moving Somnur rocks. Being sandwiched between the oppositely moving blocks of PGCF and TNF, tightening of the large scale folds within Somnur rocks occurred and they ultimately failed through development of conjugate FFZs (figure 12d). However conjugate FFZ formation was initiated at a shallower level than the basal decollement.

6.4 *A kinematic model*

Based on integrated geometric and finite strain data (figure 12) a kinematic model for the Proterozoic Somanpalli Group, including chiefly the Somnur Formation and the adjacent PGCF and TNF, has been proposed. The main tenets of this model are:

- The Somnur rocks were buckle shortened over a regional decollement separating the basement granitoid/gneiss from the overlying sedimentary succession (Saha 1992a and b). Adjoining belts of PGCF and TNF also suffered fold and thrust shortening at the same time. Some degree of cleavage shortening accompanied folding.
- Extensional stage normal faults separating shallow water sequences (the SF) from the deeper water sequences (TNF and PGCF) were reactivated and thrust mode shortening became prevalent at this stage.
- Tightening of folds within Somnur rocks occurred under the influence of oppositely moving thrust blocks (PGCF and TNF) from two sides and they failed through development of oppositely dipping sets of inclined FFZs on the flanks of antiforms.
- Strike slip regime ensued with the development of conjugate strike slip faults consistent with the shortening associated with major fold-and-thrust structures.

7. Conclusions

Minor structures and their overprinting relationships indicate that deformation within Somnur rocks was characterized by three sequentially younger structural stages: folding, thrusting and conjugate strike slip faulting. The geometry of interacting minor and large-scale fold-and-thrusts, the pattern of along strike variation in FFZs and thrusts suggests that folding and thrusting were kinematically linked processes. However the nature of variation of mesoscopic fabric over large folds and finite strain data constrain folds to have developed through fixed hinge buckling. As a result the extant models of asymmetric fold developments in thrust belts, *viz.*, fault bend or fault propagation fold models which rely heavily on hinge migration and passive fold growth with increasing slip within kink band boundaries, seem less likely to be applicable in Somnur fold-and-thrust belt. Domainal variation in finite strain exists within rocks of the Somnur Formation; low strain zones characterized by approximately irrotational flattening type deformation produced upright folds and cleavage whereas high strain zones along FFZs and thrusts are marked by inclined cleavage and folds involving strong localized noncoaxial deformation. The observed structures are best explained by large scale buckle folding above a subsurface decollement. Detachment folding is important in thin skinned deformation of sedimentary successions above a (high grade) gneissic basement. The asymmetric nature of large scale folds indicate that bulk deformation was achieved through a combination of pure and simple shear. The FFZs and smaller thrusts are second order structures that form at higher structural levels and not connected with the basal decollement. But these were developed in conjugate sets and formed later with respect to the large folds.

Acknowledgements

Financial and infrastructure support for the field work was provided by Indian Statistical Institute, Kolkata by way of funding the project "Tectonic setting of Proterozoic sediments around Somanpalli, PG valley". The initial work was done while GG was in receipt of a junior research fellowship

at ISI, Kolkata. GG also acknowledges the Department of Geology, Presidency College, Kolkata for providing UGC-SAP infrastructural facilities. The authors are also grateful to two anonymous reviewers for a critical review of the earlier version of the manuscript.

References

Anastasio D J, Fischer D M, Messina T A and Holl J E 1997 Kinematics of de'collement folding in the Lost River Range, Idaho; *J. Struct. Geol.* **19** 355–368.

Butler R W H 1989 The influence of pre-existing basin structure on thrust system evolution in the western Alps; In: Inversion Tectonics, (eds) M H Cooper and G D Williams, *Geol. Soc. Spec. Publ.* **44** 105–122.

Chaudhuri A and Chanda S K 1991 The Proterozoic basin of Pranhita–Godavari valley: an overview; In: Sedimentary basins of India: Tectonic Context, (eds) S K Tandon, C C Pant and S B Casshyap (Nainital: Ganodaya Prakashan) Pp. 13–30.

Chaudhuri A K, Saha D, Deb G, Patranabis Deb S, Mukherjee M K and Ghosh G 2002 The Purana basins of southern cratonic province of India – a case for Mesoproterozoic fossil rifts; *Gond. Res.* **5** 23–33.

De Paor D G 1988 Rf-φ strain analysis using an orientation net; *J. Struct. Geol.* **10** 323–333.

De Sitter L U 1956 *Structural Geology* (London: McGraw-Hill) p. 552.

Donath F A and Parker R B 1974 Folds and folding; *Geol. Soc. Am. Bull.* **75** 45–62.

Dunnet D W 1969 A technique of finite strain analysis using elliptical particles; *Tectonophysics* **7** 117–136.

Escher A and Watterson J 1974 Stretching fabrics, folds and crustal shortening; *Tectonophysics* **22** 223–231.

Etheridge M A 1986 On the reactivation of extensional fault systems; *Philos. Trans. R. Soc. London* **A317** 179–194.

Evans M A and Dunne W M 1991 Strain factorization and partitioning in the North Mountain thrust sheet, central Appalachians, U.S.A; *J. Struct. Geol.* **13** 21–35.

Fischer M P, Woodward N B and Mitchell M M 1992 The kinematics of break-thrust folds; *J. Struct. Geol.* **14** 451–460.

Fischer M P and Anastasio D J 1994 Kinematic analysis of a large scale leading edge fold, Lost River Range, Idaho; *J. Struct. Geol.* **16** 337–364.

Ghosh G 1997 Fold-fault relations and cleavage development at shallow crustal level in the intra-cratonic Proterozoic belt near Godavari–Indravati confluence, S. India. Unpublished Ph.D. thesis. Calcutta University, p. 305.

Ghosh G and Saha D 1999 Deformation of the Proterozoic Somanpalli Group, Pranhita–Godavari Valley – implications for a Mesoproterozoic basin inversion; Abs. In: Geology of the Pranhita–Godavari Valley: Current Status and Future Directions, Pp. 14–16.

Ghosh G and Saha D 2003 Deformation of the Proterozoic Somanpalli Group, Pranhita–Godavari valley, South India – implication for a Mesoproterozoic basin inversion; *J. Asian Earth Sci.* **21** 579–594.

Ghosh S K 1966 Experimental tests of buckling folds in relation to strain ellipsoid in simple shear deformations; *Tectonophysics* **3** 169–185.

Hedlund C A, Anastasio D J and Fisher D M 1994 Kinematics of fault-related folding in a duplex, Lost River Range, Idaho, U.S.A.; *J. Struct. Geol.* **16** 571–584.

Homza T X and Wallace W K 1995 Geometric and Kinematic models for detachment folds with fixed and variable detachment depths; *J. Struct. Geol.* **17** 475–488.

Jackson J A 1980 Reactivation of basement faults and crustal shortening in orogenic belts; *Nature* **283** 343–346.

Jamison W J 1987 Geometric analysis of fold development in overthrust terranes; *J. Struct. Geol.* **9** 207–219.

Mawer C K and Williams P F 1991 Progressive folding and foliation development in a sheared coticule bearing phyllite; *J. Struct. Geol.* **13** 539–555.

Naqvi S M and Rogers J J W 1987 Precambrian Geology of India (New York: Oxford University Press) p. 223.

Poblet J and McClay K 1996 Geometry and kinematics of single layer detachment folds; *Am. Assoc. Petrol. Geol. Bull.* **80** 1085–1109.

Price N J 1967 The initiation and development of asymmetric buckle folds in non-metamorphosed competent sediments; *Tectonophysics* **4** 173–201.

Price N J and Cosgroove J W 1990 Analysis of Geological Structures (New York: Cambridge University Press) p. 502.

Ramberg H 1964 Selective buckling of composite layers with contrasted rheological properties, a theory for the formation of several orders of folds; *Tectonophysics* **1** 307–341.

Ramsay J G 1967 Folding and fracturing of rocks (New York: McGraw-Hill) p. 568.

Ramsay J G and Huber M I 1987 Techniques of Modern Structural Geology: 2. Folds and fractures (London: Academic Press) p. 307.

Robin P Y F 1977 Determination of geologic strain using randomly oriented strain markers of any shape; *Tectonophysics* **42** T7–T16.

Saha D 1989 The Caledonian Skerrols thrust, SW Scotland – microstructure and strain; *J. Struct. Geol.* **11** 553–568.

Saha D 1990 Internal geometry of a thrust sheet, eastern Proterozoic belt, Godavari vallet, south India; *Proc. Indian Acad. Sci.* **99** 339–355.

Saha D 1992a Contractional deformation of a faulted sedimentary prism; *Ind. J. Geol.* **64** 365–376.

Saha D 1992b Geologic constraints on depths of tectonic mobility in a Proterozoic intracratonic basin; *Ind. Min.* **46** 259–270.

Saha D and Ghosh G 1998 Lithostratigraphy of deformed Proterozoic rocks from around the confluence of the Godavari and Indravati rivers, South India; *Ind. J. Geol.* **70** 217–230.

Sanderson D J 1979 The transition from upright to recumbent folding in the Variscan fold belt of southwest England: a model based on the kinetics of simple shear; *J. Struct. Geol.* **1** 171–180.

Sanderson D J 1982 Models of strain variation in nappes and thrust sheets: a review; *Tectonophysics* **88** 201–233.

Skjernaa L 1980 Rotation and deformation of randomly oriented planar and linear structures in progressive simple shear; *J. Struct. Geol.* **2** 101–109.

Stewart K G and Alvarez W 1991 Mobile-hinge kinking in layered rocks and models; *J. Struct. Geol.* **13** 243–259.

Suppe J 1983 Geometry and kinematics of fault-bend folding; *Am. J. Sci.* **283** 684–721.

Suppe J and Medwedeef D A 1990 Geometry and kinematics of fault-propagation folding; *Eclogae Geol. Helv.* **83** 409–454.

Suppe J, Sabat F, Munoz J, Poblet J, Roca E and Verges J 1997 Bed-by-bed fold growth by kink-band migration:

Sant Llorenc de Morunys, eastern Pyre'ne'es; *J. Struct. Geol.* **19** 443–461.

Tavarnelli E 1997 Structural evolution of foreland fold-and-thrust belt: Umbria-Marche Apennines, Italy; *J. Struct. Geol.* **19** 523–534.

Thorbjornsen K L and Dunne W M 1997 Origin of a thrust related fold: geometric *vs.* kinematic tests; *J. Struct. Geol.* **19** 303–319.

Turner F J and Weiss L E 1963 *Structural analysis of metamorphic tectonites* (New York: McGraw Hill) p. 545.

Twiss R J and Moores E M 1992 *Structural Geology* (New York: W.H. Freeman) p. 532.

White S H, Bretan P G and Rutter E H 1986 Fault zone reactivation: Kinematics and mechanism; *Philos. Trans. R. Soc. London* **A137** 81–97.

Williams G D, Powell C M and Cooper M A 1989 Geometry and kinematics of inversion tectonics; In: Inversion Tectonics, (eds) M H Cooper and G D Williams, *Geol. Soc. Spec. Publ.* **44** 3–15.

Willis B 1893 Mechanics of Appalachian structure; *U S Geol. Surv. Annual Report* **13** 217–281.

Zapata T R and Allmendinger R W 1996 Growth stratal records of instantaneous and progressive limb rotation in the Precordillera thrust belt and Bermejo basin, Argentina; *Tectonics* **15** 1065–1083.

MS received 13 August 2004; accepted 23 November 2004